Identification of *Meloidogyne panyuensis* on Orah and its influence on rhizosphere soil microbial characteristics from Guangxi, China (#90099)

First submission

Guidance from your Editor

Please submit by **1 Nov 2023** for the benefit of the authors (and your token reward) .

Structure and Criteria
Please read the 'Structure and Criteria' page for general guidance.

Raw data check
Review the raw data.

Image check
Check that figures and images have not been inappropriately manipulated.

If this article is published your review will be made public. You can choose whether to sign your review. If uploading a PDF please remove any identifiable information (if you want to remain anonymous).

Files

Download and review all files from the materials page.

7 Figure file(s)
2 Table file(s)
2 Other file(s)

Structure your review

The review form is divided into 5 sections. Please consider these when composing your review:

1. **BASIC REPORTING**
2. **EXPERIMENTAL DESIGN**
3. **VALIDITY OF THE FINDINGS**
4. General comments
5. Confidential notes to the editor

You can also annotate this PDF and upload it as part of your review

When ready submit online.

Editorial Criteria

Use these criteria points to structure your review. The full detailed editorial criteria is on your guidance page.

BASIC REPORTING

- Clear, unambiguous, professional English language used throughout.
- Intro & background to show context. Literature well referenced & relevant.
- Structure conforms to PeerJ standards, discipline norm, or improved for clarity.
- Figures are relevant, high quality, well labelled & described.
- Raw data supplied (see PeerJ policy).

EXPERIMENTAL DESIGN

- Original primary research within Scope of the journal.
- Research question well defined, relevant & meaningful. It is stated how the research fills an identified knowledge gap.
- Rigorous investigation performed to a high technical & ethical standard.
- Methods described with sufficient detail & information to replicate.

VALIDITY OF THE FINDINGS

- Impact and novelty not assessed. *Meaningful* replication encouraged where rationale & benefit to literature is clearly stated.
- All underlying data have been provided; they are robust, statistically sound, & controlled.
- Conclusions are well stated, linked to original research question & limited to supporting results.

Standout reviewing tips

The best reviewers use these techniques

Tip	*Example*
Support criticisms with evidence from the text or from other sources	*Smith et al (J of Methodology, 2005, V3, pp 123) have shown that the analysis you use in Lines 241-250 is not the most appropriate for this situation. Please explain why you used this method.*
Give specific suggestions on how to improve the manuscript	*Your introduction needs more detail. I suggest that you improve the description at lines 57- 86 to provide more justification for your study (specifically, you should expand upon the knowledge gap being filled).*
Comment on language and grammar issues	*The English language should be improved to ensure that an international audience can clearly understand your text. Some examples where the language could be improved include lines 23, 77, 121, 128 – the current phrasing makes comprehension difficult. I suggest you have a colleague who is proficient in English and familiar with the subject matter review your manuscript, or contact a professional editing service.*
Organize by importance of the issues, and number your points	*1. Your most important issue* *2. The next most important item* *3. …* *4. The least important points*
Please provide constructive criticism, and avoid personal opinions	*I thank you for providing the raw data, however your supplemental files need more descriptive metadata identifiers to be useful to future readers. Although your results are compelling, the data analysis should be improved in the following ways: AA, BB, CC*
Comment on strengths (as well as weaknesses) of the manuscript	*I commend the authors for their extensive data set, compiled over many years of detailed fieldwork. In addition, the manuscript is clearly written in professional, unambiguous language. If there is a weakness, it is in the statistical analysis (as I have noted above) which should be improved upon before Acceptance.*

Identification of *Meloidogyne panyuensis* on Orah and its influence on rhizosphere soil microbial characteristics from Guangxi, China

Xiaoxiao zhang [Equal first author, 1], **Wei Zhao** [Equal first author, 1], **Bin Shan** [2], **Shanshan Yang** [Corresp. 1]

[1] Guangxi Key Laboratory of Agro-Environment and Agric-Products safety, College of Agriculture, Guangxi University, Nanning, China

[2] Guangxi Subtropical Crops Research Institute, Key Laboratory of Quality and Safety Control for Subtropical Fruit and Vegetable, Ministry of Agriculture and Rural Affairs, Nanning, China

Corresponding Author: Shanshan Yang
Email address: yangshanshan12@126.com

Recently, root-knot nematode disease has severely affected the yield and quality of Orahs in Guangxi, China. However, the pathogen is poorly understood, and the effect of this disease on microbial communities requires further exploration. This study identified the root-knot nematode *Meloidogyne panyuensis* in the rhizosphere of infected Orah based on morphological and molecular biological methods. Soil chemical properties showed that the organic matter, total nitrogen (TN), total phosphorus (TP), available phosphorus (AP), total potassium (TK), and available potassium (AK) were significantly higher in *M. panyuensis*-infected Orah rhizosphere soil than those of healthy ones. The relative abundances of *Bacillus*, *Sphingomonas*, and *Burkholderia-Caballeronia-Paraburkholderia* bacteria were higher in *M. panyuensis*-infected rhizosphere soil, whereas the relative abundances of *Lycoperdon*, *Fuasrium*, *Neocosmospora*, *Talaromyces*, and *Tetragoniomyces* fungi were higher in *M. panyuensis*-infected rhizosphere soil. Furthermore, organic matter, TN, available nitrogen (AN), TP, AP, TK, and AK positively correlated with bacterial communities (*Burkholderia-Caballeronia-Paraburkholderia*, *Bacillus*, and *Sphingomonas*) and fungal communities (*Lycoperdon*, *Fuasrium, Neocosmospora*, *Talaromyces*, and *Tetragoniomyces*) in *M. panyuensis*-infected Orah rhizosphere soil. Potential root-knot nematode control strains were identified by comparing the differences in rhizosphere microbial composition between healthy Orah and *M. panyuensis*-infected Orah. This laid a foundation for early warning and prevention of root-knot nematode disease in Orah.

Identification of *Meloidogyne panyuensis* on Orah and its influence on rhizosphere soil microbial characteristics from Guangxi, China

Xiaoxiao Zhang [1#], Wei Zhao [1#], Bin Shan [2], Shanshan Yang [1*]

[1] Guangxi Key Laboratory of Agro-Environment and Agric-Products safety, College of Agriculture, Guangxi University, Nanning, 530004, China

[2] Guangxi Subtropical Crops Research Institute, Key Laboratory of Quality and Safety Control for Subtropical Fruit and Vegetable, Ministry of Agriculture and Rural Affairs, Nanning, 530001, China

[*] Corresponding author:

Shanshan Yang[1]

No.100, East Daxue Road, Xixiangtang District, Nanning, Guangxi, China

Email address: yangshanshan12@126.com

[#]These authors contributed equally to this study.

Abstract

Recently, root-knot nematode disease has severely affected the yield and quality of Orahs in Guangxi, China. However, the pathogen is poorly understood, and the effect of this disease on microbial communities requires further exploration. This study identified the root-knot nematode *Meloidogyne panyuensis* in the rhizosphere of infected Orah based on morphological and molecular biological methods. Soil chemical properties showed that the organic matter, total nitrogen (TN), total phosphorus (TP), available phosphorus (AP), total potassium (TK), and available potassium (AK) were significantly higher in *M. panyuensis*-infected Orah rhizosphere soil than those of healthy ones. The relative abundances of *Bacillus*, *Sphingomonas*, and *Burkholderia-Caballeronia-Paraburkholderia* bacteria were higher in *M. panyuensis*-infected rhizosphere soil, whereas the relative abundances of *Lycoperdon*, *Fuasrium*, *Neocosmospora*, *Talaromyces*, and *Tetragoniomyces* fungi were higher in *M. panyuensis*-infected rhizosphere

soil. Furthermore, organic matter, TN, available nitrogen (AN), TP, AP, TK, and AK positively correlated with bacterial communities (*Burkholderia-Caballeronia-Paraburkholderia*, *Bacillus*, and *Sphingomonas*) and fungal communities (*Lycoperdon*, *Fuasrium, Neocosmospora*, *Talaromyces*, and *Tetragoniomyces*) in *M. panyuensis*-infected Orah rhizosphere soil. Potential root-knot nematode control strains were identified by comparing the differences in rhizosphere microbial composition between healthy Orah and *M. panyuensis*-infected Orah. This laid a foundation for early warning and prevention of root-knot nematode disease in Orah.

Keywords: Orah; Root-knot nematode; *Meloidogyne panyuensis*; Rhizosphere soil; Microbiome

Introduction

Citrus was first cultivated in China, and both the planting area and yield are far ahead of those in the world. The Guangxi Zhuang Autonomous Region has become one of the main citrus-producing areas in China owing to its unique natural conditions and abundant labor resources. The planting area of citrus in Guangxi is stable at approximately 53.3×10^5 hm^2, and the yield exceeds 0.11×10^8 t. It is the leading industry for local farmers to remove poverty. Increases in market demand and prices have led to the expansion of citrus planting areas in recent years.

Wuming district of Nanning City (Guangxi Zhuang Autonomous Region) has vigorously developed the Orah industry, increased policy support, strengthened scientific and technological support, strictly controlled product quality and safety, vigorously conducted brand creation, and focused on brand effects to drive product marketing. This production base drives product processing and promotes the development of the entire industrial chain of Orahs. In 2022, the planting area of Wuming Orah reached 30,700 hm^2, the yield reached 1.5 million tons, and the annual output value exceeded 10 billion yuan. This region is now the largest Orah production area in China.

The expansion of cultivated areas has increased the occurrence of citrus disease (especially root nematode disease); this restricts the yield and quality of citrus. Citrus root-knot nematodes mainly infect new citrus roots and enlarge new root tips or form root knots of varying sizes that cannot elongate normally. The aboveground part of the plant is short, the leaves are short, leaves gradually yellow and fall off, and the top twigs wilt. Fourteen types of root-knot nematodes harm

citrus, and different regions have different species of root-knot nematodes, such as *Meloidogyne incognita* and *M. javanica* in Jiangxi province (Liao et al., 1990), and *M. panyuensis* in Sichuan province (He et al., 2020). Root-knot nematode diseases have rapidly spread with the adjustment of agricultural structure and the development of mechanized production, and their occurrence has increased annually. This situation is complex and ever-changing and often involves multiple diseases and nematodes. It is crucial to identify pathogenic nematodes and develop targeted prevention and control measures to ensure the stable development of the Orah industry.

Microorganisms in the soil rhizosphere form symbiotic relationships with the host, and the soil rhizosphere microbiome is important for plant health (Tsang et al., 2020). Abiotic and biotic factors cause dynamic changes in soil rhizosphere microbial communities. Soil chemical properties depend on microbes can influence plant health (Ma et al., 2022). *Pseudomonas fluorescens* 2-79RN$_{10}$ protects wheat against take-all disease, and the biocontrol activity of *P. fluorescens* 2-79RN$_{10}$ is assisted by the content of Zn and organic matter (Ownley et al., 2003). Moreover, soil chemical properties influence the soil microbial community and cause soil-borne diseases (Li et al., 2022). For example, soil pH and the C to N ratio can affect the microbial community of the rhizosphere soil and further influence plant health (Hogberg et al., 2007; Janvier et al., 2007). *Phellinus noxius* infection affects the rhizosphere microbiome of archaea and fungi (Tsang et al., 2020), and native microbial flora in wilted soil is highly suppressive (Joshi et al., 2021). In addition, the soil rhizosphere soil microbial compositions between healthy and diseased plants were obviously different. Healthy watermelons have the lowest abundance of *Fusarium oxysporum* and pH, and the highest ammonium and nitrate contents (Meng et al.,

2019). However, there is no research on the citrus rhizosphere microbiome in relation to nematode infection.

Plant growth promoting rhizobacteria (PGPR) are important components of the plant rhizosphere soil microbial community and are a major biocontrol microbial resource. They can effectively reduce damage to plants caused by environmental stress, maintain the stability of the soil microbial community structure, and significantly antagonize pathogen growth (Zhang et al., 2020). Many independent studies have depicted Proteobacteria as dominant members of the rhizosphere microbiota, such as bacteria from the Pseudomonadaceae or Burkholderiaceae family (Philippot et al., 2013). Orah is a hybrid with a high yield, good flavor, and superior quality, and has become the fastest growing late-maturing citrus variety in China (Jiang and Cao, 2011; Qiu et al., 2022). Orahs infected with root-knot nematodes exhibit weak growth that reduces yield and quality. In this study, the pathogen of Orah root-knot nematode disease in Guangxi was identified. Through the analysis of the changes of microbial community in the soil where the disease occurred, combined with the related network analysis of soil chemical properties, rhizosphere microbial community and disease occurrence, the potential bacterial genus related to the occurrence of the disease was found. It is important to prevent and control the root-knot nematode disease, increase yield, reduce environmental pollution, and maintain sustainable development of Orah agriculture.

Materials & methods

Sample collection

Samples of Orah roots and rhizosphere soil used in this study were collected in June 2022 in

Wuming District, Nanning City, Guangxi Zhuang Autonomous Region (22°58′45.92″N, 108°11′51.24″E). The healthy Orah samples were marked as CRH, while the root-knot-infected Orah samples were marked as CRN. Egg samples were extracted from the root knots of Orah, purified and inoculated in the roots of disease-susceptible hollow-beetle in sterilized soil for propagation. Second-stage juveniles (J2s) were collected from hatching eggs. Triplicate rhizosphere soil samples were collected 5 cm below the soil surface around the trees to avoid surface contamination. The roots were carefully exposed and the attached soil was sampled with a small shovel. The soil samples were stored in a cooler and transported to the laboratory. The rhizosphere soil was divided into two parts: 1) preserved at -80 °C to determine the rhizosphere soil microbial communities; 2) air-dried to determine soil chemical properties. Simultaneously, the fruits of healthy and nematode-infected Orahs were collected to evaluate their mass and diameter.

Nematode extraction and identification

Female adults were selected from Orah root-knot tissue under an anatomical microscope, and a slide consisting of 45% lactic acid solution was used to make an impression of the perineal pattern. The tail end of the nematode was cut with a scalpel, and the eggs and other adhesions attached to the inside were carefully removed and slightly modified with a brush, leaving only the perineal pattern part. The perineal pattern was transferred to a glass slide with one drop of pure glycerol, covered with a cover glass, and photographed under an optical microscope (Yang et al., 2021).

One single clean J2s nematode was placed into a 500 μL centrifuge tube, and 8 μL ddH2O

and 1 μL 10× PCR buffer was added. The tube was placed in liquid nitrogen for 1 min, then heated to 85℃ for 2 min, and this process was repeated 7-8 times. Then, 1 μL 1 mg/mL proteinase K was added, followed by incubation at 56℃ for 1 h and 95℃ for 10 min. This nematode genomic DNA was directly used for PCR or stored at -20℃. The rDNA-ITS sequence of the root-knot nematodes was amplified using the universal primers: V5367/26S (5'-TTGATTACGTCCCTGCCCTTT-3'; 5'- TTTCACTCGCCGTTACTAAGG-3') (Vrain, 1993) using the extracted DNA as a template. The obtained rDNA-ITS sequences were compared to other sequences using BLAST (NCBI) and analyzed using the neighbor-joining method with MEGA 6.0 software. The PCR reaction system was performed as followed: 2 μL DNA template, 2 μL of each primer, 25 μL of 2×Rapid Taq Master Mix, and 21 μL ddH2O. The PCR reaction procedure included initial denaturation at 95℃ for 3 min, followed by 35 cycles of 95℃ for 30 s, 55℃ for 30 s, and 72℃ for 30 s, and a final extension step at 72℃ for 5 min, followed by storage at 4℃. The PCR products were examined and sequenced. In addition, specific primers were used to detect nematodes: Mp-F/Mp-R (5'-GTTTTCGGCCCGCAACATGT-3' and 5'-CACCGCCTTGCGTAAACTCC-3'). The PCR reaction system was described above. The PCR reaction procedure included initial denaturation at 95℃ for 3 min followed by 30 cycles of 95℃ for 30s, 63℃ for 30s, 72℃ for 45s, and a final extension at 72℃ extension 5 min, stored at 4℃. Amplification products were examined by 1% agarose gel electrophoresis for the appearance of a single band as expected 409 bp (He et al., 2020).

Healthy Orah seedlings were purchased from the Guangxi Subtropical Crops Research Institute and transplanted into the sandy loam soil. After survival, 1000 J2s nematodes were

inoculated into the roots, which were routinely managed at room temperature. The root soil was removed after three months to observe the damage caused by nematodes to the roots of the Orah.

Soil chemical properties

The chemical properties of soil pH, organic matter, total nitrogen (TN), available nitrogen (AN), total phosphorus (TP), available phosphorus (AP), total potassium (TK), and available potassium (AK) were determined as described previously (Bao, 2000). Soil pH was determined using a composite glass electrode meter with a soil: water ratio of 1:2.5. Soil TN was determined using the semi-micro Kjeldahl method, soil AN was determined using a Kjeldahl nitrogen meter, soil TP and AP were determined using the molybdenum-antimony anti-colorimetric method, and soil TK and AK were determined using the flame photometric method.

Soil DNA isolation and PCR conditions

Total DNA was extracted from each rhizosphere soil sample (0.4 g) using the MoBio PowerSoil kit according to the manufacturer's instructions. The purity and concentration of the extracted DNA were quantified by a Nanodrop spectrophotometer (ND-2000) and on 0.5% agarose gels. Bacterial communities were determined using the universal forward primer (338F:5'-ACTCCTACGGGAGGCAGCAG-3') and reverse primer (806R:5'-GGACTACHVGGGTWTCTAAT-3') to amplify the 16S rRNA gene (Guo et al., 2019). Fungal communities were examined using the universal forward primer (ITS1F:5'-CTTGGTCATTTAGAGGAAGTAA-3') and reverse primer (ITS2R:5'-GCTGCGTTCTTCATCGATGC-3') to amplify the ITS1 gene (Li et al., 2020). The PCR reactions were performed in a 20 μL volume containing 4 μL of 5×FastPfu Buffer, 2 μL of 2.5

mM dNTPs, 0.8 μL of each primer, 0.4 μL FastPfu Polymerase, 0.2 μL bovine serum albumin (BSA), 10 ng soil genomic DNA, and ddH_2O to 20 μL. Amplifications were performed using an initial denaturation step of 95℃ for 3 min, followed by 30 cycles of denaturation at 95℃ for 30 s, annealing at 50℃ for 30 s, and extension at 72℃ for 45 s; with a final extension step at 72℃ for 7 min, then stored at 4℃. The PCR products were purified with a PCR Clean-Up™ kit (MO BioLabs) and sent to the Majorbio Company (Shanghai, China) for sequencing using an Illumina MiSeq PE300 (Edgar, 2013).

High-throughput sequencing analysis

The raw sequenced sequences were quality-controlled (QC) using fastp software (https://github.com/OpenGene/fastp, version 0.20.0) (Chen et al., 2018), and spliced using FLASH software (http://www.cbcb.umd.edu/software/flash, version 1.2.7) (Magoc and Salzberg, 2011): filtering bases with quality values below 20 at the end of the reads, setting a window of 50 bp, truncating back-end bases from the window if the average quality value within the window was below 20, filtering reads below 50 bp after QC, and removing reads containing N bases. The pairs of reads were spliced (merged) into one sequence with a minimum overlap length of 10 bp according to the overlap relationship between pair end double-end sequencing reads; the maximum mismatch ratio in the overlap region of the spliced sequence was 0.2, and the non-conforming sequences were screened; the samples were distinguished according to the barcode and primers at the beginning and end of the sequence, and the sequence orientation was adjusted. The number of mismatches of the barcode was 0 and the maximum number of primer mismatches was 2. The data were used for subsequent bioinformatics analyses.

All data analyses were performed using the Meguiar BioCloud platform (https://cloud.majorbio.com). Alpha diversity Coverage, and Chao 1, Simpson, Shannon, and Sobs indices were calculated using mothur software (http://www.mothur.org/wiki/Calculators), and the Wilxocon rank sum test was used to analyze group differences in Alpha diversity and to complete the dilution curve analysis; the similarity of microbial community structure between samples was examined using principal coordinate analysis (PCoA) based on the Bray-Curtis distance algorithm; the analysis of microbial community composition was performed with python software (https://www.python.org); the Wilxocon rank sum test, two-tailed test, bootstrap algorithm for microbial community inter-group variation and Bray-Curtis distance algorithm for correlation with environmental factors were performed by R-3.3.1 software (https://www.r-project.org/).

Statistical analysis

IBM SPSS Statistics 20 was used to analyze significant differences in the growth indicators (the mass and diameter of Orah), soil chemical properties, and ecological indicators (Coverage, Chao1, Simpson, and Shannon indices).

Results

Rot-knot nematode infection decreased the yield of Orah

In June, investigation found that the growth of many Orah, which was infected by root-knot nematode, was very weak. Compared with healthy roots, the roots infected by nematodes had root knots of different sizes, and the root disks were together to form fibrous roots, which were messy (Fig 1A, B). The mass and diameter of fruits were significantly lower in rot-knot

nematode infected Orah than in healthy Orah (Fig 1C). The average diameter of root-knot nematode infected Orah was 3.86 cm, which the average mass of healthy Orah was 2.95 cm, the average mass of root-knot nematode infected Orah reduced 23.58% than that of healthy Orah (Fig 1D). The average mass of root-knot nematode infected Orah was 7.49 g, which the average diameter of healthy Orah was 19.48 g, the average diameter of root-knot nematode infected Orah reduced 61.55% than that of healthy Orah (Fig 1E).

Identification of rot-knot nematode infecting Orah

There was slight variation among individuals in the female perineal pattern population, but the degree of variation among populations was similar. Microscopic observation of root-knot nematode populations isolated from Orah showed that the root-knot nematode was *M. panyuensis*: the female was white, spherical to pear-shaped, with obvious neck, and the neck ring was clear. The back ring was not obvious, the excretory orifice was located at the median bulb. The pin was developed, and the basal knob was thick. The perineal pattern was oval, the line was smooth, the back arch was low, and there was no obvious side line (Fig 2A). The morphology of the nematode was consistent with that previously reported. (He et al., 2020).

The length of the obtained rDNA-ITS sequence was 869-870 bp (GenBank accession numbers OR135523-OR135524), Blast results confirmed that those sequences were 97.59-99.08% identical to those of *M. panyuensis* from *Arachis hypogaea* L. in Guangdong, China (AY394719.1)(Liao et al., 2005). The phylogenetic tree based on the rDNA-ITS sequences was constructed, and the results showed that *M. panyuensis* of Guangxi was clustered with the *M. panyuensis* of Guangdong (AY394719.1) (Liao et al., 2005) within a group at a value of 100%

(Fig 2B). A single 409 bp specific fragment was obtained by PCR amplification using the DNA of root-knot nematodes as template and specific primers Mp-F/Mp-R of *M. panyuensis* (Fig 2C).

The inoculation of cultured J2s into healthy Orah seedlings with good growth, and culturing at room temperature for 3 months. It was found that the inoculated roots produced root knots (Fig 2D, E).

Soil chemical properties

Infection with *M. panyuensis* did not significantly affect the pH but had a great influence on the organic matter, TN, AN, TP, AP, TK, and AK (Table 1). The organic matter, AP, AK, TN, TP, and TK significantly increased in *M. panyuensis*-infected Orah rhizosphere soil by 58.87%, 14.39%, 521.39%, 37.14%, 52.31%, and 30.34%, respectively compared with healthy Orah rhizosphere soil.

General analyses of the sequencing data

The V3-V4 region of bacterial 16S rDNA and fungal ITS high-throughput sequencing results of Orah rhizosphere soil samples were analyzed, and 348051 and 382559 optimized sequences were obtained, respectively. Furthermore, 3509 and 1085 amplicon sequence variant (ASV) sets were generated using the clustering method. The cluster analysis of the ASVs set covered over 99 % of the Orah rhizosphere soil microorganisms. This indicated that the sequencing results reflected the changes in the citrus rhizosphere soil microbial community. The dilution curve of Shannon and Sobs indices tended to be gentle with increasing sequencing depth (Fig S1). This indicated that the sequencing depth was sufficient to reflect the vast majority of soil bacteria and fungi. In

addition, from the ecological index, coverage, it could also reflect that the current sequencing depth was sufficient to cover more than 99 % of soil bacteria and fungi (Table 2).

Soil bacterial and fungal diversities

The diversity of bacterial and fungal communities in healthy Orah rhizosphere soils was compared with *M. panyuensis*-infected soils. The community richness index (Chao1 index) and community diversity (Shannon index) in *M. panyuensis*-infected Orah soil increased for bacteria, whereas community diversity (Simpson index) decreased. Meanwhile, the Chao1 and Shannon indices in *M. panyuensis*-infected Orah soil decreased for fungi, whereas the Simpson index increased. However, there was no significant difference between the healthy and *M. panyuensis*-infected Orah rhizosphere soils (Table 2). The *M. panyuensis*-infected Orah rhizosphere soil bacterial community was separated from healthy Orah rhizosphere soil bacterial community according to PCoA; the combined horizontal and vertical axes in the figure explained 70.6%; the ANalysis of SIMilarity (ANOSIM) discriminant coefficient R was 0.1852 (Fig 3A). However, the result was not significantly different ($P>0.05$). The *M. panyuensis*-infected Orah rhizosphere soil fungal community partly overlapped with the healthy Orah soil bacterial community; the combined horizontal and vertical axes in the figure explained 68.6%, the ANOSIM discriminant coefficient R was 0.3704, but $P>0.05$ (Fig 3B). Therefore, this was also not significantly different. These results showed that there was no significant difference in rhizosphere soil community diversity between healthy and *M. panyuensis*-infected Orah rhizosphere soils.

Soil bacterial and fungal taxonomic composition

The *M. panyuensis*-infected Orah rhizosphere soil and the healthy plant rhizosphere soil had the

same bacterial community composition, and 229 orders were detected. Among them, the relative abundances of Rhizobiales, Burkholderiales, Acidobacteriales, Bacillales, Sphingobacteriales, Bryobacterales, Vicinamibacterales, Frankiales, and Chitinophagales, Ktedonobacterales, Gaiellales, and Xanthomonadales were all above 2%, and were the dominant bacteria in Orah rhizosphere soil. The abundances of the remaining 217 orders were below 2%. The abundance of Burkholderiales in *M. panyuensis*-infected Orah soil (63%) was significantly higher than the 37% in healthy Orah soil (Fig 4A). In total, 609 genera were identified. Among them, *Bacillus, Bryobacter*, *Sphingomonas*, *Acidothermus*, *Burkholderia-Caballeronia-Paraburkholderia*, *norank-f-norank-o-Acidobacteriales*, *norank-f-norank-o-Vicinamibacterales*, *norank-f-norank-o-Gaiellales* and *norank-f-Xanthobacteraceae* accounted for over 2%, and were the dominant bacteria in Orah rhizosphere soil. The abundances of the other 600 genera were below 2%. The abundance of *Burkholderia-Caballeronia-Paraburkholderia* in *M. panyuensis*-infected Orah soil was 84% (Fig 4B). This was significantly higher than the 16% in healthy Orah soil. These results indicate that *Burkholderia-Caballeronia-Paraburkholderia* were closely related to the occurrence of nematode disease.

M. panyuensis-infected Orah rhizosphere soil and healthy Orah rhizosphere soil had the same fungal community composition, and 11 phyla were detected. Among these, the relative abundances of Ascomycota, Basidiomycota, unclassified_k_Fungi, Rozellomycota, and Mortierellomycota were above 1%, and were the dominant phyla in the rhizosphere soil. The abundances of the other six phyla were below 1%. The abundance of Basidiomycota in *M. panyuensis*-infected Orah rhizosphere soil was 81%; this was significantly higher than the 19%

in healthy Orah rhizosphere soil (Fig 4C). A total of 275 genera were identified. Among these, *Lycoperdon*, *Roussoella*, *Fusarium*, *Neocosmospora*, *Penicillium*, *Chaetomium*, *Talaromyces*, *Acrocalymma*, *unclassified_k_Fungi*, and *Tetragoniomyces* accounted for over 3%, whereas the remaining 265 genera accounted for below 3%. The abundance of *Lycoperdon* phylum in *M. panyuensis*-infected Orah rhizosphere soil was 99%; this was significantly higher than the 1% in healthy Orah rhizosphere soil (Fig 4D). This indicated that there was a connection between *Lycoperdon* and the occurrence of nematode disease.

Comparative analysis between groups of healthy and *M. panyuensis*-infected Orah soil microbial communities

Comparative analysis of bacteria in Orah rhizosphere soil samples showed that the relative abundance of *Burkholderia-Caballeronia-Paraburkholderia* in *M. panyuensis*-infected Orah soil was 4.71%. This was 5.44-fold greater than that in healthy Orah rhizosphere soil groups (0.87%). The relative abundance of *Bacillus* in *M. panyuensis*-infected Orah rhizosphere soil was 5.53%; this was 1.40-fold greater than that in healthy Orah rhizosphere soil group (3.96%). The relative abundance of *Sphingomonas* in *M. panyuensis*-infected Orah rhizosphere soil was 3.75%; this was 1.50-fold greater than that in healthy Orah rhizosphere soil groups (2.50%) (Fig 5A). This further indicated a relationship between *Burkholderia-Caballeronia-Paraburkholderia, Bacillus, Sphingomonas*, and nematode diseases.

Comparative analysis of fungi in Orah rhizosphere soil samples showed that the relative abundance of *Lycoperdon* in *M. panyuensis*-infected Orah rhizosphere soil was 19.55%; this was 77.01-fold greater than that in healthy Orah rhizosphere soil groups (0.2506%). The relative

abundance of *Fuasrium* in *M. panyuensis*-infected Orah rhizosphere soil was 11.06%; this was 1.68-fold greater than that in healthy Orah rhizosphere soil groups (6.58%). The relative abundance of *Neocosmospora* in *M. panyuensis*-infected Orah soil was 11.22%; this was 2.50-fold greater than that in healthy Orah rhizosphere soil groups (4.48%). The relative abundance of *Talaromyces* in *M. panyuensis*-infected Orah rhizosphere soil was 7.98%; this was 12.28-fold greater than that in the healthy Orah soil group (0.65%). The relative abundance of *Tetragoniomyces* in *M. panyuensis*-infected Orah rhizosphere soil was 3.79%; this was 189.50-fold greater than that in the healthy Orah rhizosphere soil group (0.02%) (Fig 5B). This further indicated that there was a relationship between *Lycoperdon*, *Fuasrium*, *Neocosmospora*, *Talaromyces*, *Tetragoniomyces*, and nematode disease.

Correlation analysis between healthy and *M. panyuensis*-infected Orah soil microbial communities and environmental factors

Redundancy analysis (RDA) showed that soil organic matter and available N, P, and K were significantly and positively correlated with the bacterial community in *M. panyuensis*-infected Orah rhizosphere soil. The explanatory degrees of the horizontal and vertical coordinates were 46.02% and 28.01%, respectively. Soil organic matter and available K showed strong correlation coefficients (r2) of 0.9982 and 0.9693, respectively (Fig 4A). Total N, P, and K were significantly positively correlated with the bacterial community in *M. panyuensis*-infected Orah rhizosphere soil. The interpretations of the horizontal and vertical coordinates were 39.05% and 27.83%, respectively. Total N and K showed a strong positive correlation, with correlation coefficients (r^2) of 0.9342 and 0.9055, respectively (Fig 4B). In addition, four of the ten genera

with the highest relative abundance were positively correlated with the bacterial community in *M. panyuensis* infected Orah rhizosphere soil, including *Burkholderia-Caballeronia-Paraburkholderia* (Fig 4A, B). This also indicated that *Burkholderia-Caballeronia-Paraburkholderia* were related to nematode infection.

The soil organic matter and available N, P, and K were significantly positively correlated with the fungal community in *M. panyuensis*-infected Orah rhizosphere soil. The horizontal and vertical coordinates were 58.18% and 20.09%, respectively. Soil organic matter showed a strong positive correlation with a correlation coefficient (r^2) of 0.9116 (Fig 4C). Total N, P, and K were significantly positively correlated with the fungal community in *M. panyuensis*-infected Orah rhizosphere soil. The interpretations of the horizontal and vertical coordinates were 47.58% and 20.74%, respectively. Among these, total P and total K showed strong positive correlations, with correlation coefficients (r^2) of 0.9031 and 0.8856, respectively (Fig 4D). In addition, four of the ten genera with the highest relative abundance were positively correlated with the fungal community in the *M. panyuensis*-infected Orah rhizosphere soil, including *Lycoperdon* (Fig 4C, D). This also indicated that *Lycoperdon* was related to nematode infection.

Discussion

Damage and identification of root-knot nematode disease in Orah

In recent years, Wuming District of Nanning City, Guangxi Zhuang Autonomous Region has vigorously developed the Orah industry, increased policy support, strengthened scientific and technological support, strictly controlled product quality and safety, vigorously carried out brand

creation, and focused on brand effect to drive product marketing. The production base drives product processing and promotes the development of the whole industrial chain of Orah. In 2022, the planting area of Wuming Orah reached 30,700 hm^2, the yield reached 1.5 million tons, and the annual output value exceeded 10 billion yuan, becoming the largest Orah production area in China. However, the disease occurs seriously during planting, and plant parasitic nematodes were one of the important pathogens on Orah, which could cause slow and declining production of Orah trees, resulting in a serious decline in yield and quality. With the adjustment of agricultural structure and the development of mechanized production, the spread of root knot nematode diseases was rapid, and the occurrence was increasing year by year. The situation was complex and ever-changing, often involving multiple diseases and nematodes. The identification of plant nematode pathogens was a prerequisite and foundation for conducting research on nematode diseases. It was crucial to quickly and accurately identify pathogenic nematodes and develop targeted prevention and control measures to ensure the stable development of the Orah industry. This study identified rot-knot nematodes collected from Orah in Wuming. Morphological and molecular biology analyses revealed that the pathogenic nematode was *M. panyuensis*. *M. panyuensis* was first isolated from peanuts in Guangzhou Province (Liao et al., 2005). This nematode was also detected in guava and pepper in Hainan, and citrus in Hunan (Rui et al., 2005; Wang et al., 2007). This was the first study showing that *M. panyuensis* harms Orah in Guangxi Zhuang Autonomous Region.

Root-knot nematode disease changed bacterial and fungal community compositions

Rhizosphere microorganisms that constitute the core of plant rhizosphere functions play important roles in plant growth and development. They are regarded as the second genome of plants and have gradually become key regulatory areas to promote green agricultural development (Zhang, 2020). Rhizosphere soil microorganisms coordinate plant growth and development by increasing the mobility of nutrients in the soil and help plants resist pathogen attacks (Cook et al., 1995; Haney et al., 2015). This study was the first to examine the effects of *M. panyuensis* on the structure and diversity of bacterial and fungal rhizosphere microbiomes in Orah. A comparison of the rhizosphere soil of root-knot nematodes and healthy Orah showed that there was no significant difference in the community diversity of bacteria and fungi in healthy rhizosphere soil and *M. panyuensis* infected rhizosphere soil samples; the effect of *M. panyuensis* infection on rhizosphere microorganisms was mainly manifested in the abundance of microbial populations.

The bacterial community in rhizosphere soil plays a key role in suppressing soil-borne plant diseases (Ling et al., 2014; Wang et al., 2017). For example, the soil bacterial community suppresses plant soil-borne diseases in developing soil upon organic fertilization, and contributes to the control of *Fusarium* sp. ACCC 36194 (Chen et al., 2020). Similarly, the bacterial community of Orahs infected with *M. panyuensis* was significantly different from that of healthy Orahs and corresponded to increased disease severity. At the order level, the relative abundances of Vicinamibacterales, Frankiales, and Ktedonobacterales were significantly reduced in *M. panyuensis*-infected rhizosphere soil, whereas those of Burkholderiales, Bacillales, Sphingomonadales, and Chitinophagales greatly increased. At the genus level, the relative

abundances of *Acidothermus*, *norank_f_norank_o_Acidobacteriales*, *norank_f_norank_o_Vicinamibacterales*, *norank_f_norank_o_Gaiellales*, and *norank_f_Xanthobacteraceae* were significantly higher in healthy rhizosphere soil, whereas the relative abundances of *Bacillus*, *Sphingomonas*, and *Burkholderia-Caballeronia-Paraburkholderia* were higher in *M. panyuensis*-infected rhizosphere soil. *Acidothermus* is acidophilic, thermophilic, grows at 37–70℃, and between pH 3.5–7.0. Thermoacidic bacteria HB4 has high-temperature cellulose decomposition ability and plays an important role in composting (Ma et al., 2009) . An increase in hydrolyzed nitrogen content in hickory root soil decreased pH and significantly increased fertility (Ding et al., 2020). Furthermore, *norank_f_norank_o_Acidobacteriales* belongs to Acidobacteria, a newly identified bacterial group with degradation characteristics. It is widely present in various natural environments, accounting for 5-46% of the soil bacterial population and is second only to Proteobacteria in some plant roots and soil environments. It contains many bacteria that can produce antibiotics, enzymes, organic acids, and so on (Ellis et al., 2003; Sang-Hoon et al., 2008). The increase in *Acidothermus* and *norank_f_norank_o_Acidobacteriales* might be beneficial for the growth of Orah and may be used as a potential probiotic for root-knot nematode disease in Orah. *Bacillus* has strong stress resistance and can secrete various hydrolytic enzymes such as lipase, protease, and amylase. It can produce spores with excellent properties such as high-temperature resistance and UV radiation resistance. It has a wide antibacterial spectrum, fast reproduction, low production cost, high safety, with a wide variety of types, and is widely used in agricultural disease prevention and control (Wang et al., 2021; Kannan et al., 2022). The increase in its

relative abundance may be related to its resistance to root-knot nematode disease. *Sphingomonas* is an abundant new microbial resource that can be used to biodegrade organophosphorus compounds and readily degrades pesticides (Nneby et al., 2010; Sharp et al., 2012). The increase in its relative abundance might be related to the degradation of pesticides used to control nematode diseases. *Burkholderia* is widely distributed in the soil, water, and plant rhizosphere, and is an important biocontrol and growth-promoting bacterium. Extracellular enzymes produced by this genus can dissolve insoluble phosphorus in soil, promote plant growth, and produce a variety of secondary metabolites that inhibit different fungal diseases (El-Banna and Winkelmann, 1998; Parke and Gurian-Sherman, 2001; Wang et al., 2011; Kim et al., 2012; Gong et al., 2019). The increase in *Burkholderia* might inhibit the growth of pathogens such as *M. panyuensis*, although this requires further research.

The rhizosphere soil fungal community plays an important role in the soil ecological environment. In agricultural production, long-term monoculture and continuous cropping can lead to changes in fungal community diversity. The abundance of soil-borne disease pathogens *Fusarium* and *Guehomyces* increased, whereas that of nematocidal fungi (*Arthrobotrys*) significantly decreased (Li and Liu, 2019). Similarly, the fungal community of Orah infected with *M. panyuensis* was significantly different from that of healthy Orah and corresponded to the upregulation of disease severity. At the phylum level, the relative abundance of Ascomycota in *M. panyuensis*-infected rhizosphere soil significantly decreased, whereas that of Basidiomycota significantly increased. At the genus level, the relative abundances of *Roussoella*, *Penicillium*, *Chaetomium*, and *Acrocalymma* were significantly higher in the healthy rhizosphere soil,

whereas the relative abundance of *Lycoperdon*, *Fuasrium*, *Neocosmospora*, *Talaromyces*, and *Tetragoniomyces* were higher in *M. panyuensis*-infected rhizosphere soil. Endophytic *Penicillium* can colonize their ecological niches and protect host plants against multiple stresses; they exhibit many biological functions that can be used in agriculture, biotechnology, and pharmaceuticals(Toghueo and Boyom, 2020). *Chaetomium* has potential biocontrol ability, and its metabolites contain a variety of chemicals that can improve soil fertility and stimulate plant growth and induce plants to improve the antioxidant capacity of certain tissues to enhance disease resistance (Gao et al., 2006; Fu and Zhang, 2012). The seed dressing and soil application of *Chaetomium globosum* inhibiting *Fusarium* is as effective as the cell suspensions, and is even better than the fungicidal mixture in promoting crop growth and reducing vascular wilt incidence (Pothiraj et al., 2021). Moreover, *Acrocalymma* can suppress soil-borne fungal diseases in cucumbers (Huang et al., 2020). The increase in *Penicillium*, *Chaetomium*, and *Acrocalymma* might be a potential probiotic beneficial for the growth of Orah. *Fuasrium* (Simes et al., 2022; Sun et al., 2022) and *Neocosmospora* (Gai et al., 2011; Sun et al., 2014) are pathogens of many diseases and the increase in their abundance might be closely related to the disease compound infection. *Talaromyces* is an important biocontrol bacterium that has a hyperparasitic effect on various pathogens, and its chitinase has strong antibacterial activity (Marois et al., 1984; Madi et al., 1997; Xian et al., 2012). In this study, the increase in *Talaromyces* abundance may be related to the inhibition of *M. panyuensis*.

Correlations between environmental variables and microbial communities

Environmental variables are closely related to microbial communities (LI et al., 2023). Soil

elements affect the soil microbial composition; in turn, soil microorganisms can change soil chemical properties (Li et al., 2009). The nitrogen, phosphorus, and potassium contents in the soil are directly related to the microbial biomass of the plant rhizosphere. The carbon content of soil mainly affects the functional activity of microorganisms in the form of available carbon. Soil available nutrients can cause changes in soil bacterial and archaeal communities, and the high content of soil nitrogen promotes excessive growth of plants to a certain extent: the aboveground part grows too much, the field is closed, resistance is reduced, and it is easily infected by pathogens (Philippot et al., 2013; Tian et al., 2016).

In this study, the contents of organic matter, TN, AN, TP, AP, TK, and AK in the *M. panyuensis*-infected Orah rhizosphere soil were all higher than those in healthy rhizosphere soil. This is consistent with a previous report showing that the TN, AN, TP, AP, TK, and AK of *Fusarium* wilt-infected watermelon rhizosphere soils were higher than those of healthy rhizosphere soils (Meng et al., 2019). Furthermore, organic matter, TN, AN, TP, AP, TK, and AK were positively correlated with the bacterial communities *Burkholderia*-*Caballeronia*-*Paraburkholderia*, *Bacillus*, and *Sphingomonas* and negatively correlated with *Acidothermus*, *norank_f_norank_o_Vicinamibacterales*, *norank_f_Xanthobacteraceae*, *norank_f_norank_o_Acidobacteriales* and *norank_f_norank_o_Gaiellales* in the *M. panyuensis*-infected Orah rhizosphere soil. Organic matter, TN, AN, TP, AP, TK, and AK were all positively correlated with the fungal communities *Lycoperdon*, *Fuasrium, Neocosmospora*, *Talaromyces*, and *Tetragoniomyces*, and negatively correlated with *Roussoella*, *Penicillium*, *Chaetomium*, and *Acrocalymma* in the *M. panyuensis*-infected Orah rhizosphere soil. This study suggests that the

composition of (and changes in) rhizosphere microorganisms may be regulated by plants. Plants faced with a pathogen infection triggers a ' help-seeking ' mechanism that actively secretes secondary metabolites to change the soil chemical properties and affect the composition of root flora. The recruited flora also forms a competitive mechanism for better adaptation to the environment, resulting in the enrichment of bacteria of specific species in the rhizosphere of diseased plants.

Conclusion

The root-knot nematode of Orah was identified as *M. panyuensis*. Further analysis of soil chemical properties and the microbiome showed that there were significant differences in organic matter, TN, AN, TP, AP, TK, and microbial community composition between the *M. panyuensis* infected Orah rhizosphere soil and healthy Orah rhizosphere soil, and there was a correlation between them. A variety of potential biocontrol strains were identified to enrich the diversity of microbial biocontrol agents. These results can guide the subsequent screening of characteristic biocontrol strains and provide a scientific basis to prevent and treat root-knot nematode diseases.

Acknowledgements

This research supported by the National Natural Science Foundation of China (32202245), the Specific Research Project of Guangxi for Research Bases and Talents (Guike AD23026066, Guike AD23026099), and the China Agriculture Research System-Guangxi Citrus Innovative Research Team (nycytxgxcxtd-2021-05-03).

Declaration of Interest

The authors declare that they have no conflict of interest.

Data Availability

The following information was supplied regarding data availability: Orah rhizosphere soil microbiome was PRJNA1010647. Bacterial microbiomes of the healthy Orah rhizosphere soil were SRR25907662, SRR25907661 and SRR25907658; Bacterial microbiomes of the root-knot-infected Orah rhizosphere soil were SRR25907657, SRR25907656 and SRR25907655; Fungal microbiomes of the healthy Orah rhizosphere soil were SRR25907654, SRR25907653 and SRR25907652; Fungal microbiomes of the root-knot-infected Orah rhizosphere soil were SRR25907651, SRR25907660 and SRR25907659.

Supplementary Material

Figure S1. The rarefaction analysis of all samples. A (Shannon index) and C (Sob index) were the bacterial community; B (Shannon index) and D (Sob index) were the bacterial community.

Table S1. The raw data for the diameter (Fig 1D) and the mass (Fig 1E) of fruits.

Table S2. The raw data of soil chemical properties of the healthy and *M. panyuensis*-infected Orah rhizosphere soil (Table 1).

Figure legends

Figure 1. Damage symptom of root-knot nematodes on Orah and its effect on yield. A, roots of healthy Orah. B, roots of root-knot nematodes infected Orah. C, the fruit appearance of the healthy Orah (CRH) and the root-knot nematodes infected Orah (CRN). D, the diameter of fruits. E, the mass of fruits.

Figure 2. Identification of rot-knot nematode infecting Orah. A, Perineal pattern of nematode female isolated from infected Orah root. Scale bar: 20 μm. B, phylogenetic tree based on rDNA-ITS of *Meloidogyne* spp.. C, specific amplification using the primers Mp-F/Mp-R in *M. panyuensis* isolated from infected Orah. M: DL 2000 Plus; 1-5: negative control (1. Water; 2-3. *M. incognita*; 4-5. *M. enterolobii*.); 6-13: *M. panyuensis*. D-E, the disease symptoms on Orah caused by *M. panyuensis*.

Figure 3. Principal coordinate analysis (PCoA) of bacterial (A) and fungal (B) communities based on bray-curtis distances.

Figure 4. Relationship between species and samples in rhizosphere soil of healthy and *M.*

***panyuensis*-infected.** A (order level) and B (genus level) were the bacterial community; C (phylum level) and D (genus level) were the bacterial community.

Figure 5. Comparative analysis of bacterial (A) and fungal (B) community in rhizosphere soil of healthy and *M. panyuensis*-infected.

Figure 6. Redudancy analysis (RDA) between healthy and *M. panyuensis*-infected Orah rhizosphere soil microbial communities and environmental factors. A and B were the bacterial community; C and D were the fungal community.

Table 1. Soil chemical properties of the healthy and *M. panyuensis*-infected Orah rhizosphere soil.

Table 2. Richness and diversity estimation of the 16S and ITS1 sequencing libraries in healthy and *M. panyuensis*-infected Orah rhizosphere soil.

References

Bao S, 2000. Soil and agricultural chemistry analysis. Beijing, China Agriculture Press.

Chen D, Wang X, Zhang W, Zhou Z, Ding C, Liao Y, Li X. Persistent organic fertilization reinforces soil-borne disease suppressiveness of rhizosphere bacterial community. PLANT SOIL 2020;452(1): 313-328.

Chen S, Zhou Y, Chen Y, Gu J. fastp: an ultra-fast all-in-one FASTQ preprocessor. BIOINFORMATICS 2018;34(17): i884-i890.

Cook RJ, Thomashow LS, Weller DM, Fujimoto D, Mazzola M, Bangera G, Kim DS. Molecular mechanisms of defense by rhizobacteria against root disease. Proc Natl Acad Sci U S A 1995;92(10): 4197-201.

Ding LZ, Jin J, Wang ZY, Zhou JM, Tong ZP, Zhou PS, Ma SS. Changes of soil fertility in carya cathayensis stands in major production towns of Lin'an City. Jouranl Zhejiang for science technology 2020;40(03): 45-50.

Edgar RC. UPARSE: highly accurate OTU sequences from microbial amplicon reads. NAT METHODS 2013;10(10): 996-8.

El-Banna N and Winkelmann G. Pyrrolnitrin from *Burkholderia cepacia*: antibiotic activity against fungi and novel activities against streptomycetes. J APPL MICROBIOL 1998;85(1): 69-78.

Ellis RJ, Morgan P, Weightman AJ, Fry JC. Cultivation-dependent and -independent approaches for determining bacterial diversity in heavy-metal-contaminated soil. APPL ENVIRON MICROB 2003;69(6): págs. 3223-3230.

Fu W and Zhang XY. Progress in antimicrobial mechanism of chaetomium. Chinese Agricultural Science

Bulletin 2012;28(07): 100-103.

Gai Y, Pan R, Xu D, Ji C, Deng M, Chen W. First report of soybean *Neocosmospora* stem rot caused by *Neocosmospora vasinfecta* var. *vasinfecta* in China. PLANT DIS 2011;95(8): 1031-1031.

Gao KX, Pang YD, Qin NH, Liu XG, Kang ZS. Synergistic antifungal activity of antibiotics and hydrolytic enzymes from endophytic *Chaetomium spirale* ND35. ACTA PHYTOPATHOLOGICA SINICA 2006.

Gong AD, Zhu ZY, Lu YN, Wan HY, Wu NN, Cheelo D, Gong S, Wen ST, Hou X. Functional analysis of *Burkholderia pyrrocinia* WY6-5 on phosphate solubilizing, antifungal and growth-promoting activity of Maize. Scientia Agricultura Sinica 2019;52(09): 1574-1586.

Guo D, Fan Z, Lu S, Ma Y, Nie X, Tong F, Peng X. Changes in rhizosphere bacterial communities during remediation of heavy metal-accumulating plants around the Xikuangshan mine in southern China. SCI REP-UK 2019;9(1).

Haney CH, Samuel BS, Bush J, Ausubel FM. Associations with rhizosphere bacteria can confer an adaptive advantage to plants. NAT PLANTS 2015;1(6).

He Q, Wang D, Zhang D, Liu Y, Cheng F. Identification and PCR detection of citrus root-knot nematode in Hunan Province. Plant Protection 2020.

Hogberg MN, Hogberg P, Myrold DD. Is microbial community composition in boreal forest soils determined by pH, C-to-N ratio, the trees, or all three? OECOLOGIA 2007;150(4): 590-601.

Huang L, Niu Y, Su L, Deng H, Lyu H. The potential of endophytic fungi isolated from cucurbit plants for biocontrol of soilborne fungal diseases of cucumber. MICROBIOL RES 2020;231: 126369.

Janvier C, Villeneuve F, Alabouvette C, Edel-Hermann V, Mateille T, Steinberg C. Soil health through soil disease suppression: Which strategy from descriptors to indicators? Soil Biology and Biochemistry 2007;39(1): 1-23.

Jiang D and Cao L. Introduction performance of late-maturing high-sugar hybrid citrus Orah in Chongqing. South China Fruits 2011;40(05): 33-34.

Joshi S, Jaggi V, Gangola S, Singh A, Sah VK, Sahgal M. Contrasting rhizosphere bacterial communities of healthy and wilted Dalbergia sissoo Roxb. forests. Rhizosphere 2021;17: 100295.

Kannan C, Divya M, Rekha G, Barbadikar KM, Maruthi P, Hajira SK, Sundaram RM. Whole genome sequencing data of native isolates of *Bacillus* and *Trichoderma* having potential biocontrol and plant growth promotion activities in rice - ScienceDirect. Data in Brief 2022.

Kim S, Lowman S, Hou G, Nowak J, Flinn B, Mei C. Growth promotion and colonization of switchgrass (*Panicum virgatum*) cv. *Alamo* by bacterial endophyte *Burkholderia phytofirmans* strain PsJN. BIOTECHNOL BIOFUELS 2012;5(1): 37.

Li D, Zhao B, Olk DC, Zhang J. Soil texture and straw type modulate the chemical structure of residues during four-year decomposition by regulating bacterial and fungal communities. APPL SOIL ECOL 2020;155: 103664.

Li HN, Liu WX, Da L, Wan FH, Cao YY. Invasive impacts of *Ageratina adenophora* (Asteraceae) on the changes of microbial community structure, enzyme activity and fertility in soil ecosystem. Scientia Agricultura Sinica 2009;42(11): 3964-3971.

Li J, Li S, Huang X, Tang R, Zhang R, Li C, Xu C, Su J. Plant diversity and soil properties regulate the microbial community of monsoon evergreen broad-leaved forest under different intensities of woodland use. SCI TOTAL ENVIRON 2022;821: 153565.

LI W, CHEN P, WANG Y, LIU Q. Characterization of the microbial community response to replant diseases in peach orchards. J INTEGR AGR 2023;22(4): 1082-1092.

Li WH and Liu QZ. Changes in fungal community and diversity in strawberry rhizosphere soil after 12 years in the greenhouse. J INTEGR AGR 2019(3): 11.

Liao JL, Yang WC, Feng ZX, Karssen G. Description of *Meloidogyne panyuensis* sp. n. (Nematoda: *Meloidogynidae*), parasitic on peanut (*Arachis hypogaea* L.) in China. RUSS J NEMATOL 2005(2): 13.

Liao Y, Chen X, Deng S. Preliminary study on citrus root-knot nematode disease. Acta Agriculturae Universitatis Jiangxi Ensis 1990(02): 5-9.

Ling N, Deng K, Song Y, Wu Y, Zhao J, Raza W, Huang Q, Shen Q. Variation of rhizosphere bacterial community in watermelon continuous mono-cropping soil by long-term application of a novel bioorganic fertilizer. MICROBIOL RES 2014;169(7-8): 570-578.

Ma H, Xie C, Zheng S, Li P, Cheema HN, Gong J, Xiang Z, Liu J, Qin J. Potato tillage method is associated with soil microbial communities, soil chemical properties, and potato yield. J MICROBIOL 2022;60(2): 156-166.

Ma HL, Gong ZJ, Chen H, Guo WX. Isolation, screening and identification of high-temperature cellulolytic microbes. Journal of Anhui Agricultural Science 2009;29(37): 13987-13988.

Madi L, Katan T, Katan J, Henis Y. Biological control of *Sclerotium rolfsii* and *Verticillium dahliae* by

Talaromyces flavus is mediated by different mechanisms. PHYTOPATHOLOGY 1997;87(10): 1054-1060.

Magoc T and Salzberg SL. FLASH: fast length adjustment of short reads to improve genome assemblies. BIOINFORMATICS 2011;27(21): 2957-63.

Marois JJ, Fravel DR, Papavizas GC. Ability of *Talaromyces flavus* to occupy the rhizosphere and its interaction with *Verticillium dahliae*. SOIL BIOL BIOCHEM 1984;16(4): 387-390.

Meng T, Wang Q, Abbasi P, Ma Y. Deciphering differences in the chemical and microbial characteristics of healthy and Fusarium wilt-infected watermelon rhizosphere soils. APPL MICROBIOL BIOT 2019;103(3): 1497-1509.

Nneby K, Jonsson A, Stenstrm J. A new concept for reduction of diffuse contamination by simultaneous application of pesticide and pesticide-degrading microorganisms. BIODEGRADATION 2010;21(1): 21.

Ownley BH, Duffy BK, Weller DM. Identification and manipulation of soil properties to improve the biological control performance of phenazine-producing *Pseudomonas fluorescens*. APPL ENVIRON MICROB 2003;6(69): 3333-3343.

Parke JL and Gurian-Sherman D. Diversity of the *Burkholderia cepacia* complex and implications for risk assessment of biological control strains. ANNU REV PHYTOPATHOL 2001;39: 225-58.

Philippot L, Raaijmakers JM, Lemanceau P, Van D. Going back to the roots: the microbial ecology of the rhizosphere. NAT REV MICROBIOL 2013;11(11): 789-799.

Philippot L, Raaijmakers JM, Lemanceau P, van der Putten WH. Going back to the roots: the microbial ecology of the rhizosphere. NAT REV MICROBIOL 2013;11(11): 789-799.

Pothiraj G, Hussain Z, Singh AK, Solanke AU, Aggarwal R, Ramesh R, Shanmugam V. Characterization of *Fusarium* Spp. inciting vascular wilt of tomato and its management by a chaetomium-based biocontrol consortium. FRONT PLANT SCI 2021;12.

Qiu F, Pan Z, Li L, Xia L, Huang G. Transcriptome analysis of Orah leaves in response to citrus canker infection. Journal of Fruit Science 2022;39(04): 631-643.

Rui K, Chen MC, Guo AP, Xiao TB, Xie SH, Wu FL, Liao JL. The identification of guava root-knot nematodes in Hainan province. Journal of South China Agricultural University 2005(04): 53-58.

Sang-Hoon, Lee, Jong-Ok, Ka, Jae-Chang, Cho. Members of the phylum *Acidobacteria* are dominant and metabolically active in rhizosphere soil. FEMS MICROBIOL LETT 2008;285(2): 263-269.

Sharp RE, Schultz-Jensen N, Aamand J, Srensen SR. Growth characterization and immobilization studies of

the MCPA pesticide degrader strain *Sphingomonas* sp. Erg5. 2012 Symposium of The Danish Microbiological Society. Nov 2012. Copenhagen, Denmark. 2012.

Simes D, Diogo E, Andrade ED. First Report of *Fusarium andiyazi* presence in portuguese Maize kernels. Agriculture 2022;12.

Sun Q, Xie YJ, Chen TM, Zhang JP, Laborda P, Wang SY. First report of *Fusarium avenaceum* causing canker disease on Kiwi tree in China. PLANT DIS 2022(6): 106.

Sun SL, Kim MY, Van K, Lee YH, Zhong C, Zhu ZD, Lestari P, Lee YW, Lee SH. First report of *Neocosmospora vasinfecta* var. *vasinfecta* causing soybean stem rot in south Korea. PLANT DIS 2014(98-12).

Tian Q, Yang X, Wang X, Liao C, Li Q, Wang M, Wu Y, Liu F. Microbial community mediated response of organic carbon mineralization to labile carbon and nitrogen addition in topsoil and subsoil. BIOGEOCHEMISTRY 2016;128(1-2): 125-139.

Toghueo RMK and Boyom FF. Endophytic penicillium species and their agricultural, biotechnological, and pharmaceutical applications. 3 BIOTECH 2020;10(3).

Tsang KSW, Cheung MK, Lam RYC, Kwan HS. A preliminary examination of the bacterial, archaeal, and fungal rhizosphere microbiome in healthy and *Phellinus noxius*-infected trees. MICROBIOLOGYOPEN 2020;9(10).

Vrain TC. Restriction Fragment Length Polymorphism Separates Species of the *Xiphinema americanum* Group. J NEMATOL 1993;25(3): 361-4.

Wang C, Henkes LM, Doughty LB, He M, Wang D, Meyer-Almes FJ, Cheng YQ. Thailandepsins: bacterial products with potent histone deacetylase inhibitory activities and broad-spectrum antiproliferative activities. J NAT PROD 2011;74(10): 2031-8.

Wang R, Wang T, Li EF. Research advances of biocontrol Bacillus in the field of plant diseases. Journal of Tianjin Agricultural University 2021;28(04): 71-77.

Wang R, Zhang H, Sun L, Qi G, Chen S, Zhao X. Microbial community composition is related to soil biological and chemical properties and bacterial wilt outbreak. SCI REP-UK 2017;7(1): 343.

Wang XL, Li JH, Peng DL. Cloning and sequence analysis of rDNA-ITS fragment of root-knot mematodes. Journal of Huazhong Agricultural University 2007(05): 624-628.

Xian HQ, Tang W, Zhang LQ, Li AN, Li DC. Cloning and expression of a chitinase gene tfchi1 from *Talaromyces flavus* and the antifungal activity of the recombinant enzyme. ACTA PHYTOPATHOLOGICA

SINICA 2012;42(02): 146-153.

Yang Y, Hu X, Liu P, Chen L, Peng H, Wang Q, Zhang Q. A new root-knot nematode, *Meloidogyne vitis* sp. nov. (Nematoda: *Meloidogynidae*), parasitizing grape in Yunnan. PLOS ONE 2021;16(2): e0245201.

Zhang FR. Rhizosphere microorganisms: the second genome of plants that play an important role in the green development of agriculture. Biotechnology Bulletin 2020;36(09): 1-2.

Zhang Y, Hu A, Zhou J, Zhang W, Li P. Comparison of bacterial communities in soil samples with and without tomato bacterial wilt caused by *Ralstonia solanacearum* species complex. BMC MICROBIOL 2020;20(1): 89.

Figure 1

Damage symptom of root-knot nematodes on Orah and its effect on yield.

Figure 1. Damage symptom of root-knot nematodes on Orah and its effect on yield. A, roots of healthy Orah. B, roots of root-knot nematodes infected Orah. C, the fruit appearance of the healthy Orah (CRH) and the root-knot nematodes infected Orah (CRN). D, the diameter of fruits. E, the mass of fruits.

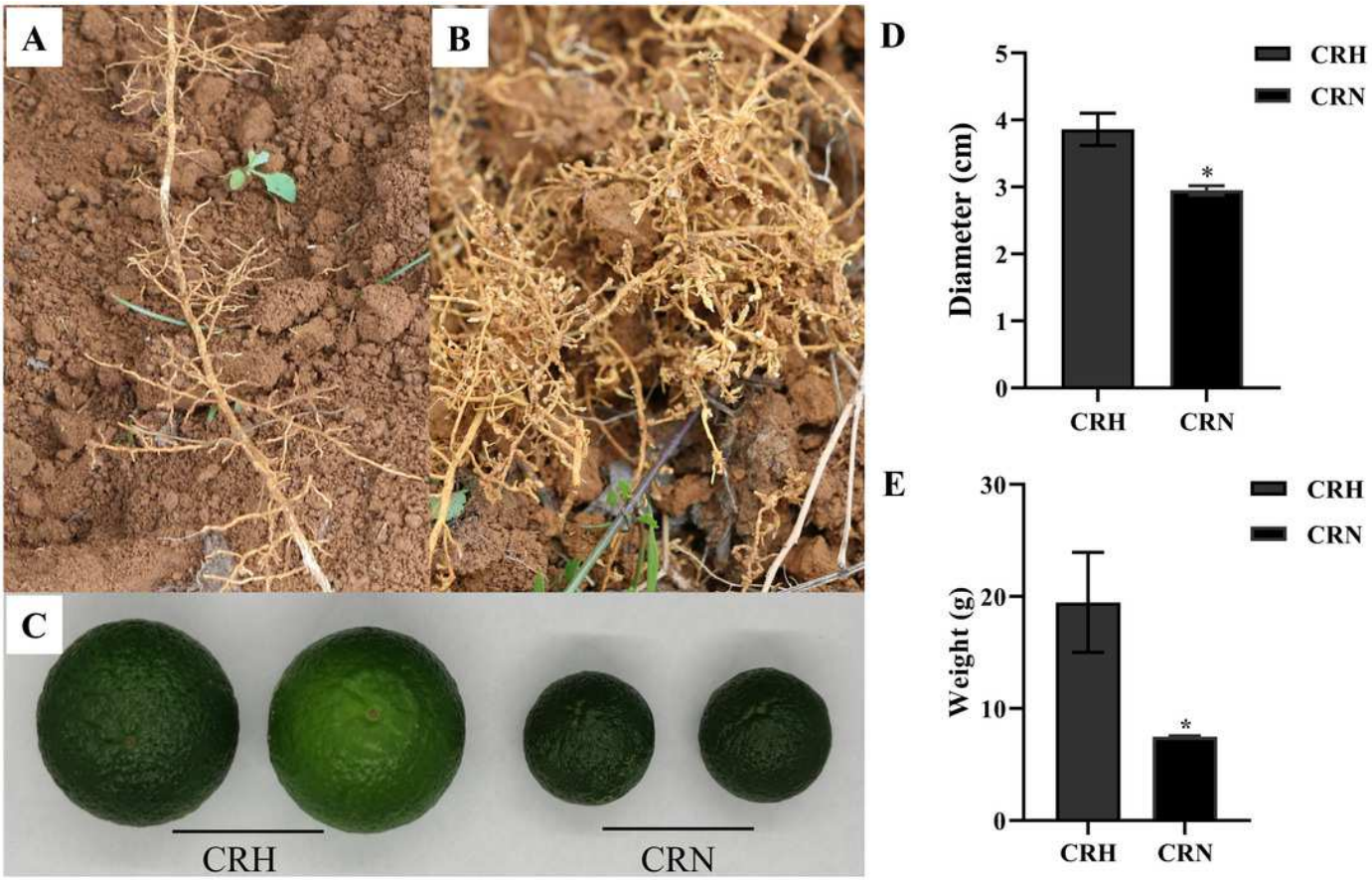

Figure 2

Identification of rot-knot nematode infecting Orah.

Figure 2. Identification of rot-knot nematode infecting Orah. A, Perineal pattern of nematode female isolated from infected Orah root. Scale bar: 20 μm. B, phylogenetic tree based on rDNA-ITS of *Meloidogyne* spp.. C, specific amplification using the primers Mp-F/Mp-R in *M. panyuensis* isolated from infected Orah. M: DL 2000 Plus; 1-5: negative control (1. Water; 2-3. *M. incognita*; 4-5. *M. enterolobii*.); 6-13: *M. panyuensis*. D-E, the disease symptoms on Orah caused by *M. panyuensis*.

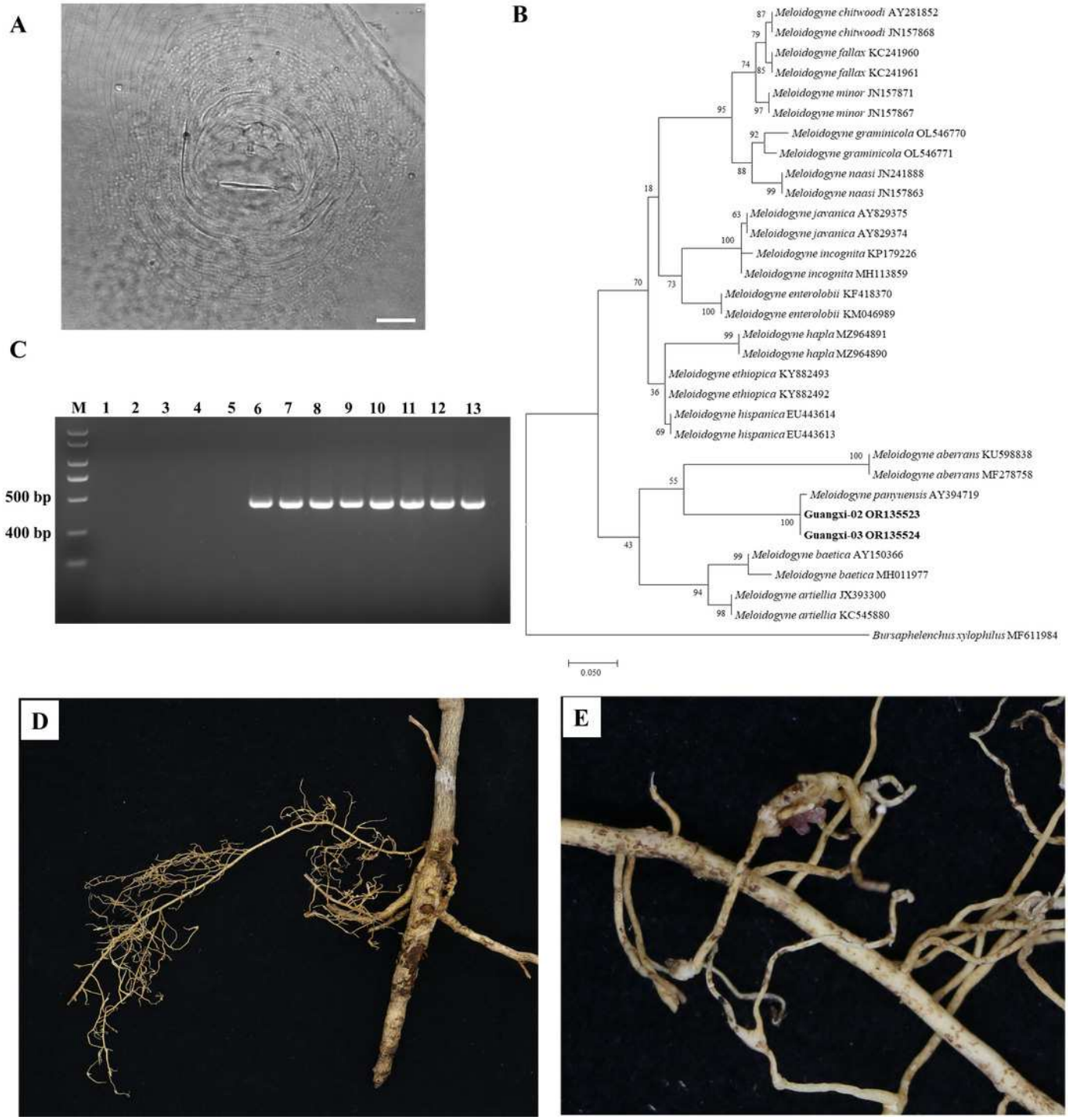
A
B
C
M 1 2 3 4 5 6 7 8 9 10 11 12 13
500 bp
400 bp
Meloidogyne chitwoodi AY281852
Meloidogyne chitwoodi JN157868
Meloidogyne fallax KC241960
Meloidogyne fallax KC241961
Meloidogyne minor JN157871
Meloidogyne minor JN157867
Meloidogyne graminicola OL546770
Meloidogyne graminicola OL546771
Meloidogyne naasi JN241888
Meloidogyne naasi JN157863
Meloidogyne javanica AY829375
Meloidogyne javanica AY829374
Meloidogyne incognita KP179226
Meloidogyne incognita MH113859
Meloidogyne enterolobii KF418370
Meloidogyne enterolobii KM046989
Meloidogyne hapla MZ964891
Meloidogyne hapla MZ964890
Meloidogyne ethiopica KY882493
Meloidogyne ethiopica KY882492
Meloidogyne hispanica EU443614
Meloidogyne hispanica EU443613
Meloidogyne aberrans KU598838
Meloidogyne aberrans MF278758
Meloidogyne panyuensis AY394719
Guangxi-02 OR135523
Guangxi-03 OR135524
Meloidogyne baetica AY150366
Meloidogyne baetica MH011977
Meloidogyne artiellia JX393300
Meloidogyne artiellia KC545880
Bursaphelenchus xylophilus MF611984
0.050
D
E

Figure 3

Principal coordinate analysis (PCoA) of bacterial (A) and fungal (B) communities based on bray-curtis distances.

Figure 3. Principal coordinate analysis (PCoA) of bacterial (A) and fungal (B) communities based on bray-curtis distances.

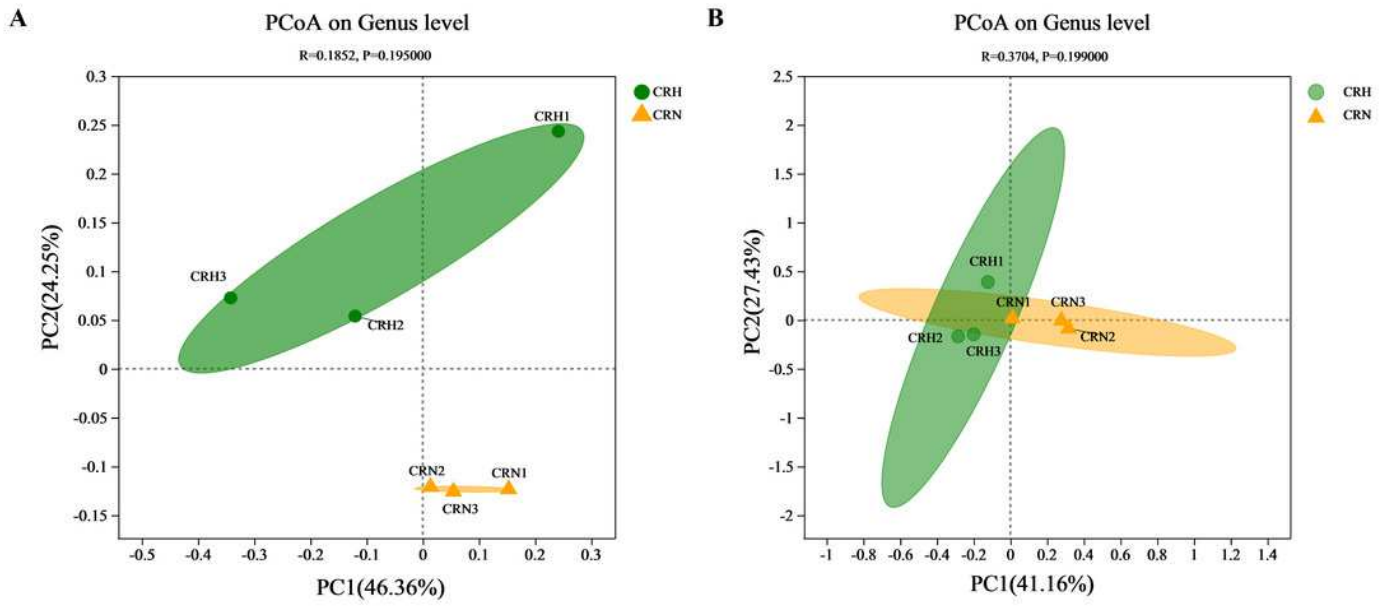

Figure 4

Relationship between species and samples in rhizosphere soil of healthy and *M. panyuensis*-infected.

Figure 4. Relationship between species and samples in rhizosphere soil of healthy and *M. panyuensis*-infected. A (order level) and B (genus level) were the bacterial community; C (phylum level) and D (genus level) were the bacterial community.

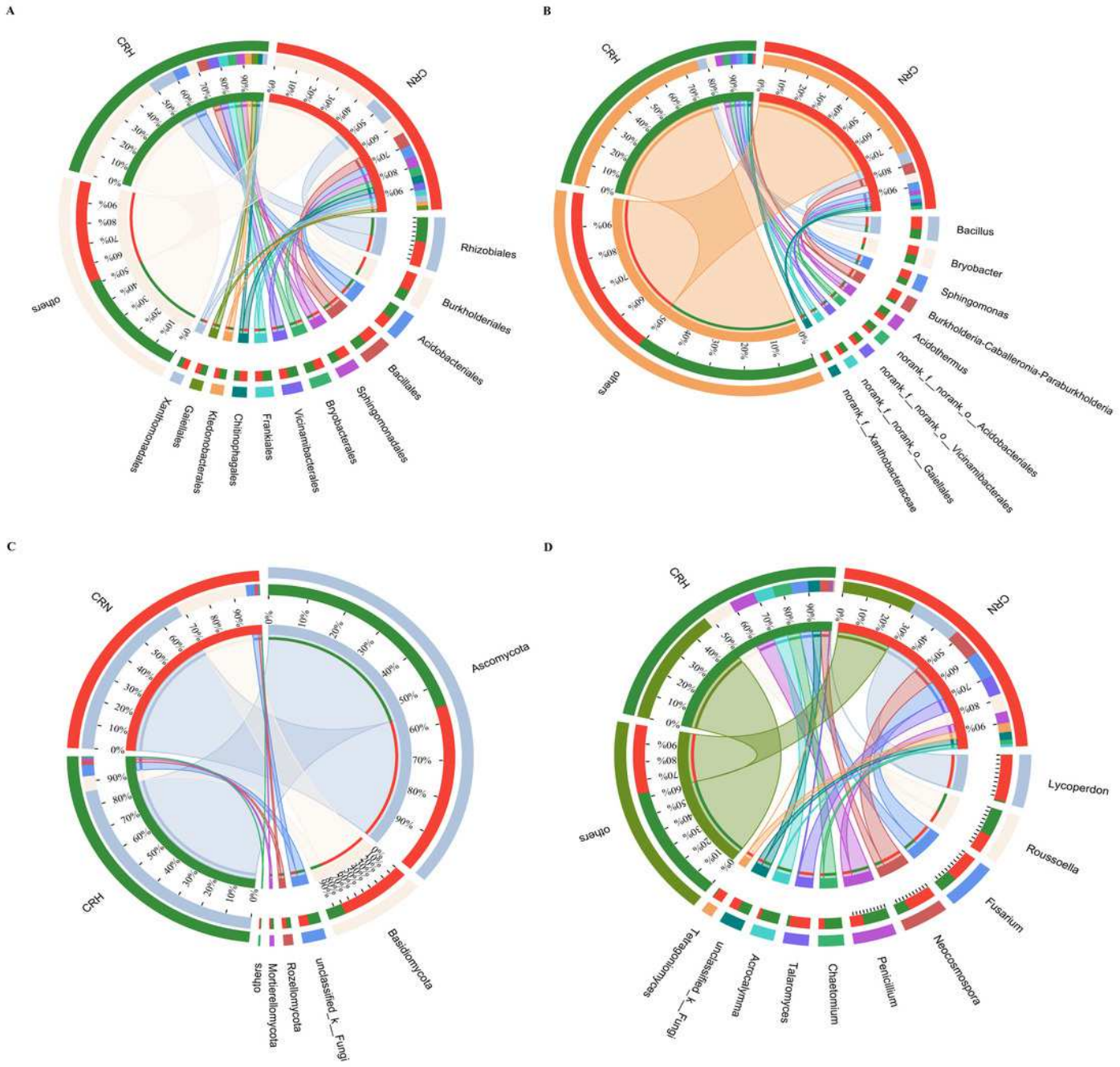
A
CRH
CRN
others
Rhizobiales
Burkholderiales
Acidobacteriales
Bacillales
Sphingomonadales
Bryobacterales
Vicinamibacterales
Frankiales
Chitinophagales
Kiteonobacterales
Gaiellales
Xanthomonadales
B
CRH
CRN
others
Bacillus
Bryobacter
Sphingomonas
Burkholderia-Caballeronia-Paraburkholderia
Acidothermus
norank_f_norank_o__Acidobacteriales
norank_f_norank_o__Vicinamibacterales
norank_f_norank_o__Gaiellales
norank_f_Xanthobacteraceae
C
CRN
CRH
Ascomycota
Basidiomycota
unclassified_k__Fungi
Rozellomycota
Mortierellomycota
others
D
CRH
CRN
others
Lycoperdon
Roussoella
Fusarium
Neocosmospora
Penicillium
Chaetomium
Talaromyces
Acrocalymma
unclassified_k__Fungi
Tetragonomyces

Figure 5

Comparative analysis of bacterial (A) and fungal (B) community in rhizosphere soil of healthy and *M. panyuensis*-infected.

Figure 5. Comparative analysis of bacterial (A) and fungal (B) community in rhizosphere soil of healthy and *M. panyuensis*-infected.

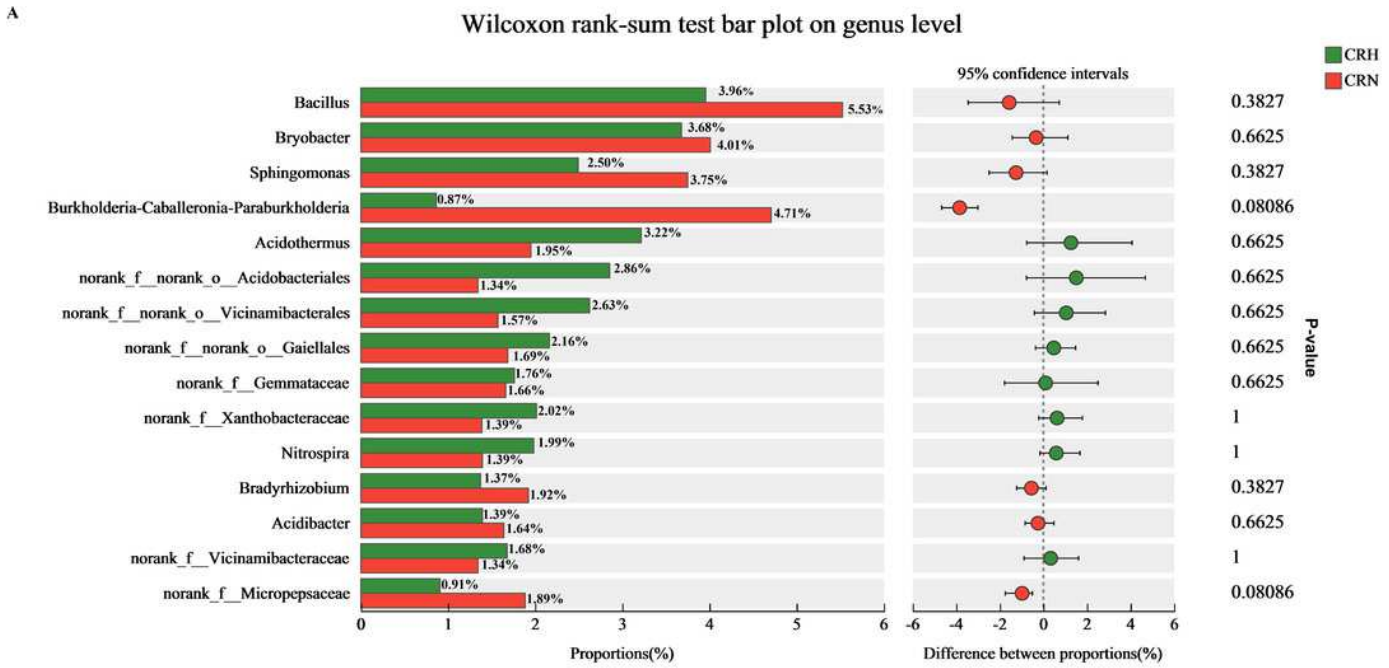
A
Wilcoxon rank-sum test bar plot on genus level
CRH
CRN
95% confidence intervals
Bacillus 3.96% 5.53% 0.3827
Bryobacter 3.68% 4.01% 0.6625
Sphingomonas 2.50% 3.75% 0.3827
Burkholderia-Caballeronia-Paraburkholderia 0.87% 4.71% 0.08086
Acidothermus 3.22% 1.95% 0.6625
norank_f__norank_o__Acidobacteriales 2.86% 1.34% 0.6625
norank_f__norank_o__Vicinamibacterales 2.63% 1.57% 0.6625
norank_f__norank_o__Gaiellales 2.16% 1.69% 0.6625
norank_f__Gemmataceae 1.76% 1.66% 0.6625
norank_f__Xanthobacteraceae 2.02% 1.39% 1
Nitrospira 1.99% 1.39% 1
Bradyrhizobium 1.37% 1.92% 0.3827
Acidibacter 1.39% 1.64% 0.6625
norank_f__Vicinamibacteraceae 1.68% 1.34% 1
norank_f__Micropepsaceae 0.91% 1.89% 0.08086
P-value
0 1 2 3 4 5 6
Proportions(%)
-6 -4 -2 0 2 4 6
Difference between proportions(%)

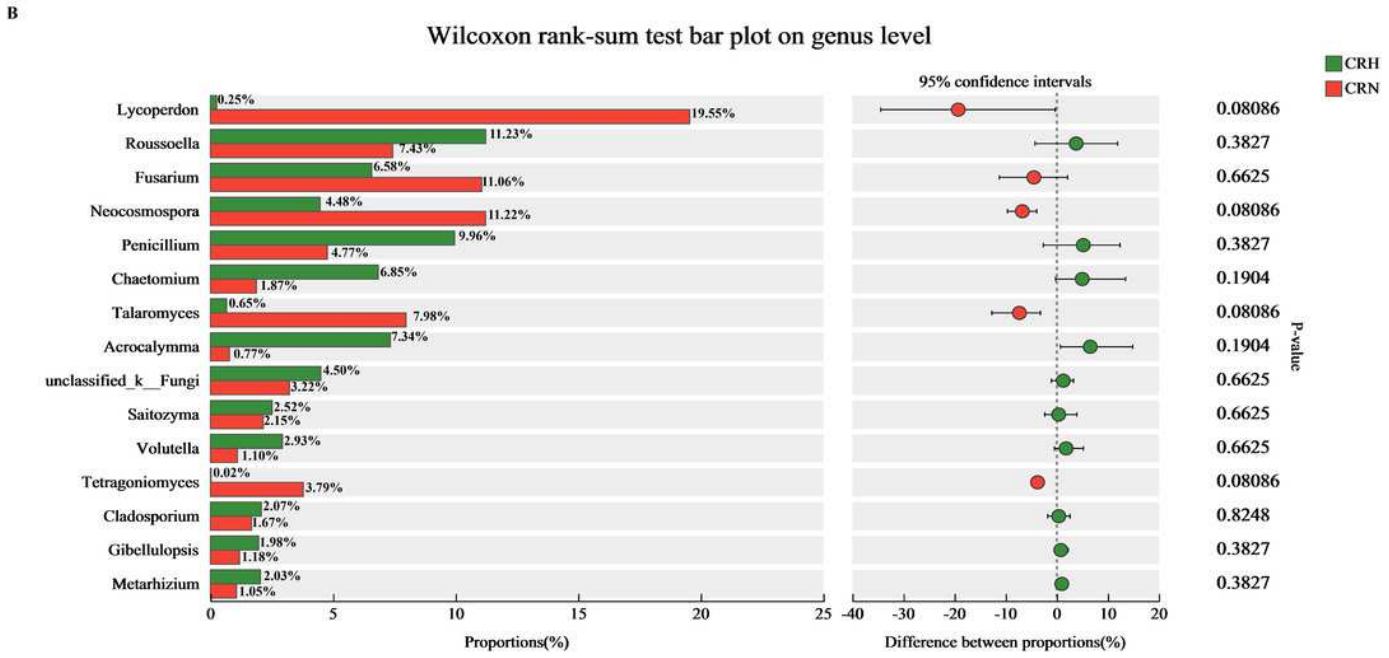
B
Wilcoxon rank-sum test bar plot on genus level
CRH
CRN
95% confidence intervals
Lycoperdon 0.25% 19.55% 0.08086
Roussoella 11.23% 7.43% 0.3827
Fusarium 6.58% 11.06% 0.6625
Neocosmospora 4.48% 11.22% 0.08086
Penicillium 9.96% 4.77% 0.3827
Chaetomium 6.85% 1.87% 0.1904
Talaromyces 0.65% 7.98% 0.08086
Acrocalymma 7.34% 0.77% 0.1904
unclassified_k__Fungi 4.50% 3.22% 0.6625
Saitozyma 2.52% 2.15% 0.6625
Volutella 2.93% 1.10% 0.6625
Tetragoniomyces 0.02% 3.79% 0.08086
Cladosporium 2.07% 1.67% 0.8248
Gibellulopsis 1.98% 1.18% 0.3827
Metarhizium 2.03% 1.05% 0.3827
P-value
0 5 10 15 20 25
Proportions(%)
-40 -30 -20 -10 0 10 20
Difference between proportions(%)

Figure 6

Redudancy analysis (RDA) between healthy and *M. panyuensis*-infected Orah rhizosphere soil microbial communities and environmental factors

Figure 6. Redudancy analysis (RDA) between healthy and *M. panyuensis*-infected Orah rhizosphere soil microbial communities and environmental factors. A and B were the bacterial community; C and D were the fungal community.

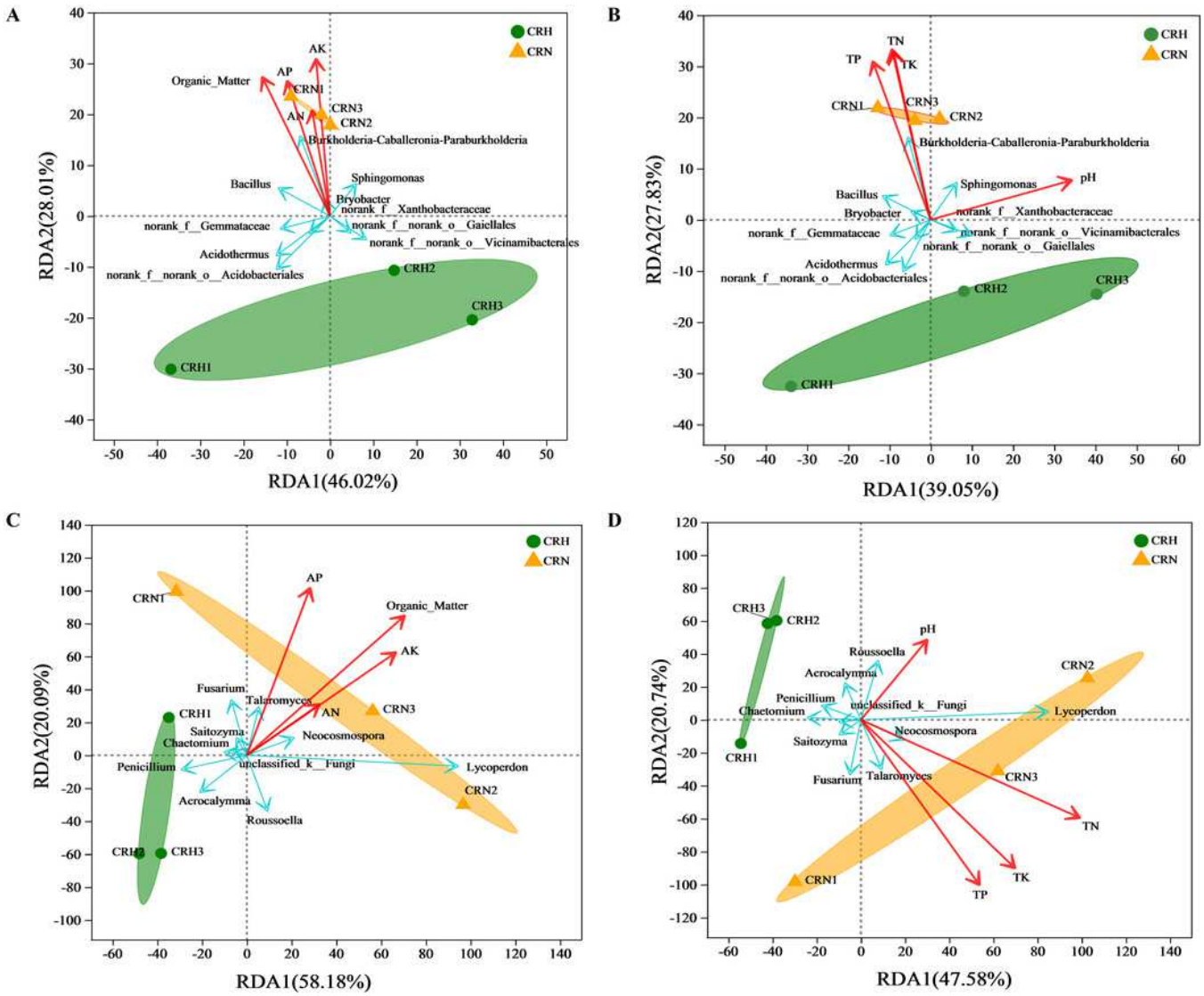

Table 1(on next page)

Soil chemical properties of the healthy and *M. panyuensis*-infected Orah rhizosphere soil.

Table 1. Soil chemical properties of the healthy and *M. panyuensis*-infected Orah rhizosphere soil.

Table 1. Soil chemical properties of the healthy and *M. panyuensis*-infected Orah rhizosphere soil.

Number	Samples	pH	Organic matter (g/kg)	AN (mg/kg)	AP (mg/kg)	AK (mg/kg)	TN (g/kg)	TP (g/kg)	TK (g/kg)
1	CRH	5.02±0.94 a	23.10±4.70 a	123.95±25.55 a	44.56±28.04 a	215.42±68.84 a	1.40±0.13 a	1.30±0.07 a	2.34±0.04 a
2	CRN	5.06±0.20 a	36.70±1.21 b	141.79±3.66 a	276.89±128.40 b	430.40±26.75 b	1.92±0.06 b	1.98±0.25 b	3.05±0.20 b

Table 2 (on next page)

Richness and diversity estimation of the 16S and ITS1 sequencing libraries in healthy and *M. panyuensis*-infected Orah rhizosphere soil.

Table 2. Richness and diversity estimation of the 16S and ITS1 sequencing libraries in healthy and *M. panyuensis*-infected Orah rhizosphere soil.

Table 2. Richness and diversity estimation of the 16S and ITS1 sequencing libraries in healthy and *M. panyuensis*-infected Orah rhizosphere soil.

Category	Group	Coverage	Chao 1	Simpson	Shannon
Bacteria	CRH	0.9996	840±77 a	0.003±0.0003 a	6.26±0.07 a
	CRN	0.9992	937±133 a	0.0025±0.0003 a	6.39±0.14 a
Fungi	CRH	1	370±75 a	0.0469±0.0093 a	3.98±0.1 a
	CRN	1	262±35 a	0.0761±0.02 a	3.5±0.29 a